PH-Triggered Reversible Multiple Protein-Polymer Conjugation Based on Molecular Recognition

ARTICLE *in* THE JOURNAL OF PHYSICAL CHEMISTRY B · AUGUST 2015

Impact Factor: 3.3 · DOI: 10.1021/acs.jpcb.5b06637 · Source: PubMed

5 AUTHORS, INCLUDING:

Juan Liu

University of Basel

4 PUBLICATIONS **6** CITATIONS

SEE PROFILE

Viktoriia Postupalenko

University of Basel

15 PUBLICATIONS **148** CITATIONS

SEE PROFILE

THE JOURNAL OF PHYSICAL CHEMISTRY B

Article

pubs.acs.org/JPCB

pH-Triggered Reversible Multiple Protein−Polymer Conjugation Based on Molecular Recognition

Juan Liu, Viktoriia Postupalenko, Jason T. Duskey, Cornelia G. Palivan,* and Wolfgang Meier*

Department of Chemistry, University of Basel, Klingelbergstrasse 80, Basel 4056, Switzerland

Supporting Information

ABSTRACT: Polymer conjugation for protein-based therapeutics has been developed extensively, but it still suffers from conjugation leading to decrease in protein activity and generates complexes with limited diversity due to general classical systems only incorporating one protein per each complex. Here we introduce a site-specific noncovalent protein−polymer conjugation, which can reduce the heterogeneity of the conjugates without disrupting protein function, while allowing for the modulation of binding affinity and stability, affecting the pH dependent binding of the number of proteins per polymer. We compared classical one protein−polymer conjugates with multiple protein−polymer conjugates using His-tagged enhanced yellow fluorescence protein (His_6-eYFP) and metal-coordinated tris-nitrilotriacetic acid (trisNTA-Me^{n+}) in a site-specific way. trisNTA-Me^{n+}-His_6 acts as a reversible linker with pH-triggered release of functional protein from the trisNTA-functionalized copolymers. The nature of the selected Me^{n+} and number of available trisNTA-Me^{n+} on poly(*N*-isopropylacrylamide-*co*-tris-nitrilotriacetic acid acrylamide) (PNT*n*) copolymers enables predictable modulation of the conjugates binding affinity (0.09−1.35 μM), stability, cell toxicity, and pH responsiveness. This represents a promising platform that allows direct control over the properties of multiple protein−polymer conjugates compared to the classical single protein−polymer conjugates.

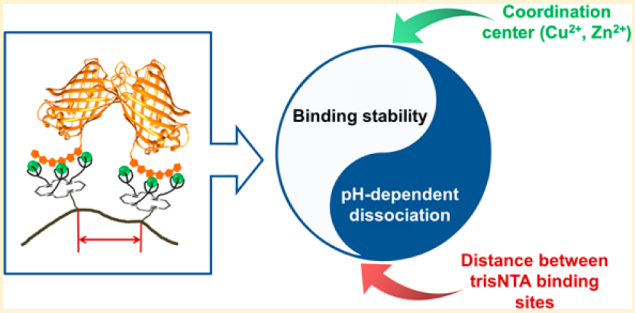

INTRODUCTION

Protein therapeutics is of high importance in almost every field of medicine.[1] However, there are still a number of challenges in the application of protein therapeutics that have to be overcome.[1,2] Therapeutic proteins exhibit low stability, fast renal clearance, enzymatic degredation, and are frequently immunogenic.[3]

An elegant way to overcome these problems is to conjugate polymers to proteins, which has been reported to improve protein stability, half-life, solubility, and reduce immunogenicity.[4−8] However, such conjugation can lead to the alteration of the protein structure, resulting in a decrease or even complete inhibition of protein activity.[9,10] An effective approach to overcome a loss of protein function is to design a stimuli-responsive linkage between polymers and proteins.[11] This enables the linkage to be independent of the protein function, and therefore, cleavage of the protein from the polymer conjugate by a specific stimulus releases the intact and functional protein.[11−13] Currently, covalent attachment of polymers to proteins through stimuli-cleavable linkers has mainly been developed.[11,13−15] Noncovalent interactions with a stimuli-responsive nature are rarely applied for protein−polymer conjugation due to their instability.[16,17] The interaction between metal-coordinated nitrilotriacetic acid (NTA-Me^{n+}) and His-tagged proteins is a promising candidate for protein−polymer conjugation, due to the binding specificity and the reversibility upon pH change or the addition of imidazole or ethylenediaminetetraacetic acid (EDTA).[18,19] Also, no modification of the protein is required as most recombinant therapeutic proteins expressed by *Escherichia coli* incorporate a His tag (His_6) for affinity purification, which can also directly coordinate the NTA-Me^{n+}. Unfortunately, to the best of our knowledge, there is only one study published using NTA-Me^{n+}-His_6 for the formation of protein−polymer conjugates for protein therapy, but the conjugates were shown to exhibit low stability due to the poor binding affinity.[16] Supramolecular entities with two or three NTA heads (bisNTA and trisNTA, respectively) exhibit improved binding affinity toward His-tagged proteins and have been used recently for the formation of protein−polymer conjugates.[16,20] Among them, trisNTA possesses the highest binding affinity,[19,21−24] but the stability and the pH-trigged releaseability of trisNTA-Me^{2+}-His_6 protein−polymer conjugates is still unknown.

Moreover, most protein−polymer conjugate systems allow for only one protein to be bound to each or multiple polymers.[7,25] Binding multiple proteins on each polymer would be able to enhance the stability of conjugates due to the

Received: July 10, 2015
Revised: August 7, 2015
Published: August 20, 2015

DOI: 10.1021/acs.jpcb.5b06637
J. Phys. Chem. B 2015, 119, 12066−12073

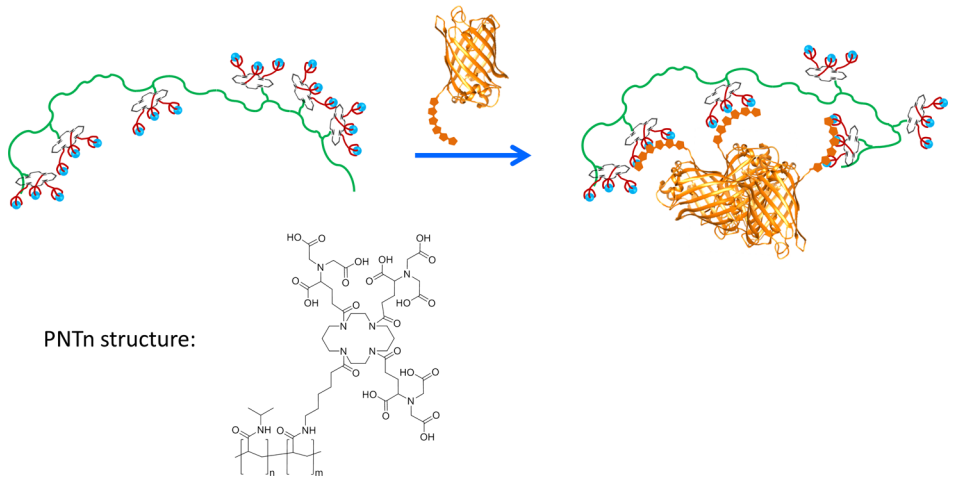

Figure 1. Schematic representation of site-specific conjugation of poly(*N*-isopropylacrylamide-*co*-tris-nitrilotriacetic acid acrylamide) polymers (green), which coordinate metals (blue) with His-tagged proteins (orange).

interprotein interactions, similar to the case of many natural stabilized protein assemblies.[26−28]

A previous study published by our group introduced poly(*N*-isopropylacrylamide-*co*-tris-nitrilotriacetic acid acrylamide) copolymers (PNT*n*, where *n* represents the mol % of trisNTA on the polymer) containing Cu^{2+} for specific binding of His-tagged molecules.[20] Here, we employed PNT*n* copolymers and His_6-eYFP (Figure 1) as models for polymer−protein conjugation to analyze the effect on the stability, pH-trigged dissociation, and toxicity when the nature of the metal, the distance between trisNTA sites, and the addition of interprotein interactions were varied. Three metal cations, Cu^{2+}, Zn^{2+}, and Fe^{3+}, were chosen as the coordination center in the trisNTA pocket to modulate the binding affinity of His-tagged proteins to the copolymers, and were assessed by isothermal titration calorimetry (ITC). Then their ability to reversibly bind on the basis of changes in pH was analyzed by fast protein liquid chromatography (FPLC). Also, the protein stability before and after conjugation, as well as after pH mediated release, were measured by circular dichroism (CD) and fluorescence spectroscopy. Our strategy of multiple protein conjugation to each polymer chain and release upon pH changes can be expanded to other systems and advance the application of noncovalent interactions for protein−polymer conjugation.

EXPERIMENTAL SECTION

Materials. Copper(II) chloride, zinc chloride, iron(III) sulfate hydrate, Dulbecco's modified eagle medium (DMEM), and phosphate-buffered saline (PBS) were purchased from Sigma-Aldrich and used as received. 3-(4,5-Dimethylthiazol-2-yl)-5-(3-(carboxymethoxy)phenyl)-2-(4-sulfophenyl)-2*H*-tetrazolium (MTS) was purchased from Promega, USA. Penicillin, streptomycin, and fetal bovine serum (FBS) were purchased from Life technologies. Rhodamine B labeled hexahistidine (RHB-His_6) was received as a gift from Dr. Thomas Schuster. Pierce BCA Protein Assay was from Thermo Scientific. All chemicals were purchased with the highest purity and used without further purification unless otherwise stated.

Chelation of Metal Cations to PNT*n* Copolymers. Respective PNT*n* copolymers (0.2 mg/mL) were dissolved in PBS, pH 7.4. A stoichiometric excess of $CuCl_2$, $ZnCl_2$, or $Fe_2(SO_4)_3$ was mixed with the respective PNT*n* solution and was purified on a HiTrap desalting column (5 mL, GE Healthcare Life Sciences) with PBS as the mobile phase.

Protein Expression and Analysis. The expression of His_6-eYFP was performed as previously published.[29] The concentration of His_6-eYFP was determined by BCA protein assay and measured absorbance at 562 nm.

CD spectra were recorded using AVIV and Applied PhotophysicsChirascan CD spectrophotometers at 25 °C with a time constant of 5 s and a step resolution of 1 nm in a 1 mm quartz cell. CD data are given as the mean of residual molar ellipticities (deg cm^2 $dmol^{-1}$). The spectra are the result of 2−4 repeats. All measured solutions contained a final concentration of 4 μM His_6-eYFP protein in PBS, where the PBS background spectrum was subtracted.

Fluorescence of 100 nM His_6-eYFP (λ_{ex} = 513 nm, λ_{em} = 524 nm) and polymer−protein conjugates was investigated with a PerkinElmer LS55 fluorescence spectrometer (Waltham, MA, USA) at ambient temperature. Fluorescence of 60 nM RHB-His_6 alone (λ_{ex} = 554 nm, λ_{em} = 585 nm) and in complex with NTA-Cu^{2+}, trisNTA-Cu^{2+}, and PNT4-Cu^{2+} was measured similarly.

Binding Ability and Affinity of His_6-eYFP to PNT*n*-Me^{n+} Copolymers. Binding stoichiometries and dissociation constants (K_D) were determined by ITC. ITC was carried out using a VP-ITC microcalorimeter from MicroCal. Interaction constants characterizing the PNT*n*-Me^{n+} copolymers and His_6-eYFP were determined by direct titration of His_6-eYFP into polymer solutions in PBS pH 7.4 at 25 °C. The concentration of His_6-eYFP and trisNTA on PNT*n* was 70 and 6 μM, respectively. During analysis the solution in the sample cell was stirred at 300 rpm. The volume of the sample cell and syringe were 1.4 mL and 295 μL, respectively. Small aliquots of His_6-eYFP (typically 10 μL) were added into the stirring solution over 240 s to allow complete equilibration. The first injection was set to a volume of 1 μL to avoid air in the syringe and ignored for data analysis. The exothermic heat pulse (upper panel, Figure S1) that corresponds to an injection of 10 μL of 70 μM His_6-eYFP to 1.4 mL of 6 μM trisNTA functional group on copolymers was recorded as a function of time. The data were analyzed using the Origin software package supplied by MicroCal and fitted by a standard single-site binding model (lower panel, Figure S1). The stoichiometry value is equal to the value of the molar ratio for which the slope of the plot in

DOI: 10.1021/acs.jpcb.5b06637
J. Phys. Chem. B 2015, 119, 12066−12073

lower panel is steepest. The slope of the plot at this point gives the value of the reciprocal of the K_D.

Stability and pH-Triggered Dissociation of PNT*n*-Me^{2+}-His$_6$-eYFP Conjugates. FPLC was used for the analysis of the stability and the pH responsiveness of PNT*n*-Me^{2+}-His$_6$-eYFP conjugates. His$_6$-eYFP (250 μM) was incubated with a metal cation-coordinated PNT*n* in PBS with a molar ratio of 1:2 for His$_6$-eYFP:trisNTA. The solution (500 μL) was loaded onto a Superdex 200 10/300 GL column (Akta Prime system, Amersham Biosciences, measuring @ 513 nm), and eluted with a PBS mobile phase. For the investigation of pH responsiveness, the column was equilibrated with PBS solution at pH 5.0 or 6.0. The sample was prepared in the same way as previously described, loaded onto the column, and eluted with PBS solution at pH 5.0 or 6.0. The data were analyzed by Fityk software to calculate the integral area of the individual peaks.

Structure of PNT*n*-Me^{2+}-His$_6$-eYFP Conjugates. The sizes of PNT*n*-Me^{2+}-His$_6$-eYFP conjugates were investigated by dynamic light scattering (DLS) with a Zetasizer Nano ZSP (Malvern Instruments Ltd., UK) at 25 °C in PBS. The data were fit on the basis of number distribution. The concentration of His$_6$-eYFP was 20 μM, and 800 μL of solution was used for measurements.

The negatively stained image of PNT4-Zn^{2+}-His$_6$-eYFP conjugates (0.1 mg/mL, 5 μL) stained with 2% uranyl acetate was performed on a transmission electron microscope (Philips CM100) at an acceleration voltage of 80 kV. The size of the conjugates was analyzed using ImageJ software.

Cell Culture. HeLa cells or U87 glioblastoma cells were maintained at 37 °C in a 5% CO_2 humidified atmosphere and were grown in DMEM with 10% FBS, 100 units/mL penicillin, 100 μg/mL streptomycin, and 2 mM L-glutamine.

Cell Viability. Cytotoxicity testing was performed using the PromegaCellTiter 96 AQueous Non-Radioactive Cell Proliferation (MTS) assay (Promega) to determine the number of viable cells in culture. HeLa and U87 cells were seeded in a 96-well plate the night before experiments at 0.5×10^4 and 1×10^4 cells/well in 100 μL, respectively. The day of the experiment, samples (10 μL) containing different amounts of PNT4-Me^{2+} (0−375 μg/mL) were added to the cells. Then, 24 h later, 20 μL of MTS solution was added to each well and incubated for 3 h at 37 °C. Cell viability was calculated by measuring the absorbance at 490 nm using a 96-well plate reader and plotted relative to untreated cells that were grown the same day in the same plate and assays were performed in triplicate.

RESULTS AND DISCUSSION

Binding Stoichiometry of His$_6$-eYFP to PNT*n* Coordinated with Different Metal Cations. PNT*n* copolymers were previously synthesized and the average distance between trisNTA binding sites of PNT1, PNT2, PNT4, and PNT7 of 31.5 nm, 13.2 nm, 5.2 and 4.3 nm, were theoretically calculated, assuming an idealized linear polymer chain, by dividing the length of the polymer chain by the corresponding average trisNTA binding sites number per chain (2, 4, 7, and 9 trisNTA per polymer, respectively) (Table S1).[20] Here we are interested to modulate the binding affinity of His-tagged proteins to these polymer chains decorated with tris-NTA groups, and in this respect, we selected three different metal cations, Cu^{2+}, Zn^{2+}, or Fe^{3+}. The binding stoichiometry of His$_6$-eYFP to the PNT-Me^{n+} was assessed by ITC to calculate the dependence of the metal and of the distance between trisNTA sites on binding stoichiometry (Figures 2 and S1). His$_6$-eYFP coordinated the

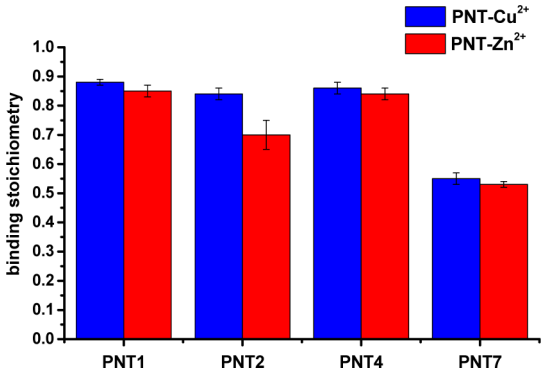

Figure 2. Binding stoichiometry between trisNTA-Me^{2+} in PNT*n* and His$_6$-eYFP.

Cu^{2+} or Zn^{2+} metals on PNT*n* copolymers with a maximum binding stoichiometry approaching 0.9:1 or 0.85:1, respectively, when the average distance between trisNTA binding sites was larger than the size of His$_6$-eYFP and steric hindrance did not block efficient binding. However, even though PNT7 has a higher content of trisNTA-Me^{2+} sites, a lower binding stoichiometry was observed (0.55 and 0.53 His$_6$-eYFP to trisNTA-Cu^{2+}and trisNTA-Zn^{2+} sites) due to steric hindrance, resulting from the coil conformation of the polymer in solution. In the case of PNT*n* containing trisNTA-Fe^{3+}, no coordination of His$_6$-eYFP was observed by ITC even when a high concentration of His$_6$-eYFP (180 μM) was added (data not shown).

Binding Affinity of His$_6$-eYFP to PNT*n*-Me^{2+} Copolymers. In addition to calculating the binding stoichiometry, the binding affinities of His$_6$-eYFP to PNT*n* containing either Cu^{2+} or Zn^{2+} were compared where the K_D value was normalized per NTA functional group per polymer chain to allow for comparison between the polymers containing different average number of binding sites. Similar to K_D values for PNT*n*-Cu^{2+} (0.09−0.39 μM), those for PNT*n*-Zn^{2+}-His$_6$-eYFP depended on the average distance between trisNTA binding sites. When the distance was decreased from 31.5 to 4.3 nm (PNT1-Zn^{2+}-His$_6$-eYFP and PNT7-Zn^{2+}-His$_6$-eYFP, respectively), the K_D values decreased from 1.35 ± 0.12 μM to 0.46 ± 0.06 μM. It is known that numerous factors play a role in the binding strength of a metal to its coordination pocket including size, charge, protein oligomerization, and other stabilizing or destabilizing interactions.[30−33] For example, increasing the number of binding sites could decrease the K_D of a small molecule due to a decreased rate of dissociation. On the contrary if the size of proteins is larger than the mean distance between trisNTA-Me^{n+} sites, the binding affinity is decreased even if an increased number of coordination is present due to steric hindrance and charge repulsion of the protein.[20] However, increasing the number of trisNTA-Me^{2+} per polymer, effectively decreasing their separation, stabilized the conjugate. Although many factors play a role in affinity, this decrease of K_D supports the previous findings that a decrease of enthalpy was seen upon binding of PNT4 compared to PNT1 copolymers, indicating an increase in hydrogen bond formation from interprotein interactions.[30−33] This led to a binding affinity dependency of PNT*n*-Me^{2+}-His$_6$-eYFP based on a combined effect between the coordination strength of the metal and the amount of interprotein interactions, which overcomes the coil hindrance (Figure 3).

DOI: 10.1021/acs.jpcb.5b06637
J. Phys. Chem. B 2015, 119, 12066−12073

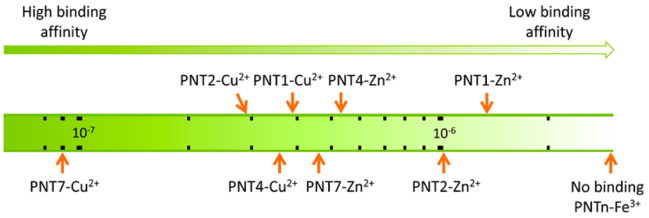

Figure 3. K_D (M) for the binding between PNT*n*-Cu^{2+}/Zn^{2+}/$Fe^{3+}$and His_6-eYFP at pH 7.4.

The binding affinity of His-tagged proteins is dependent on the strength of coordination with the metal where Cu^{2+} > Ni^{2+} > Zn^{2+} > Fe^{3+}.[34] Therefore, Zn^{2+} is rarely used for NTA conventional applications, such as purification of proteins, due to its poor binding affinity ($\log_{10} K$ = 3.25 M^{-1}).[35] Even with the increased binding created by using trisNTA instead of NTA or bisNTA, it is apparent that when interprotein interactions are not present, as is the case for PNT1, the binding affinity with Zn^{2+} is still much weaker than its Cu^{2+} equivalent. When the interprotein interaction increases as a result of an increased number of accessible trisNTA coordination pockets, the binding affinity increases due to stabilization of the conjugates. However, for PNT7 the steric hindrance leads to a decrease in binding stoichiometry as described above. Introducing interprotein interactions leads to more stable Zn^{2+} conjugates, which makes them suitable for further applications (Figure 3). This strategy is seen in nature to stabilize self-assembled structures by interprotein interactions.[26−28]

Physical Characteristics of PNT*n*-Me^{2+}-His_6-eYFP Conjugates and Protein Stability. The size of PNT*n*-Me^{2+}-His_6-eYFP conjugates was characterized by DLS. PNT1-Cu^{2+}/Zn^{2+} and PNT4-Cu^{2+}/Zn^{2+} were chosen as representative polymers for further investigations including size measurements and stabilities in various pHs. Even though PNT1 has an average number of two trisNTA-Me^{2+} binding sites per polymer, to compare a multiple protein system to the classical one protein per PNT1, a 2:1 ratio of trisNTA-Me^{2+} to His_6-eYFP was chosen. Also, because the binding studies showed a stoichiometry <1 for PNT*n* polymers to the average number of binding sites, this means each polymer solution has a mixture of polymers containing an average number of accessible binding sites less than the theoretical value (two for PNT1, and seven for PNT4). Therefore, this 2:1 ratio was used for both PNT*n* to keep the number of proteins proportional on each polymer chain. For this molar ratio, there are an average of three or four His_6-eYFPs per polymer chain for PNT4, and an average of one His_6-eYFP per polymer chain for PNT1. In addition, due to the excess of trisNTA-Me^{2+} compared to His_6-eYFP, no free proteins are expected.

To directly measure the size shift of the tertiary structure of polymer chains in solution due to the binding of proteins, dynamic light scattering was performed. The hydrodynamic diameter (D_H) of His_6-eYFP was determined to be 5.0 ± 0.9 nm. The D_H of PNT1-Zn^{2+} was 8.1 ± 2.5 nm and when coordinated with His_6-YFP increased in size to 9.7 ± 2.4 nm (Figure S3). PNT4-Zn^{2+} was 5.8 ± 1.8 nm (Figure S2), and after binding, the diameter value shifted to 13.1 ± 2.8 nm, which was similar to that of PNT4-Cu^{2+}-His_6-eYFP (data not shown). The change in size between PNT1-Zn^{2+} and PNT4-Zn^{2+} after binding His_6-eYFP can be explained by the increased average number of proteins per polymer. The DLS data were supported with transmission electron microscopy (TEM), revealing structures with a diameter of 12 ± 3 nm for PNT4-Zn^{2+}-His_6-eYFP (Figure S4).

To address the question of whether the conjugation of polymers to proteins causes alterations in their secondary structure, His_6-eYFP was characterized before and after polymer conjugation by CD spectroscopy. The far-UV CD spectra of His_6-eYFP and PNT1/4-Zn^{2+}-His_6-eYFP, showed that conjugation did not alter the protein structure (Figure S5), agreeing with the previously published results.[20,36]

PNT*n*-Me^{2+}-His_6-eYFP Stability under Varying pHs. The stability of PNT*n*-Me^{2+}-His_6-eYFP conjugates under various pH's was investigated by FPLC. Each of the protein−polymer conjugates was measured to establish a baseline of the amount of free His_6-eYFP in each and calculated as a percent of intact protein−polymer complex (Figure 4). PNT1-Cu^{2+}-His_6-eYFP showed a lower stability than PNT4-Cu^{2+}-His_6-eYFP at pH 7.4 (Figure S6). The difference between PNT1-Zn^{2+}-His_6-eYFP and PNT4-Zn^{2+}-His_6-eYFP was even more significant with only 46.6% of His_6-eYFP remaining bound with PNT1-Zn^{2+} but 80.2% of His_6-eYFP remaining complexed with PNT4-Zn^{2+}. Because PNT*n*-Me^{2+} copolymers are highly negatively charged,[20] the potential electrostatic interactions between protein−polymer conjugates and gel filtration media might decrease the stability of conjugates during the FPLC analysis.[37−39] This was tested by increasing the number of available PNT4-Zn^{2+} from 2 to 10 equiv compared to His_6-

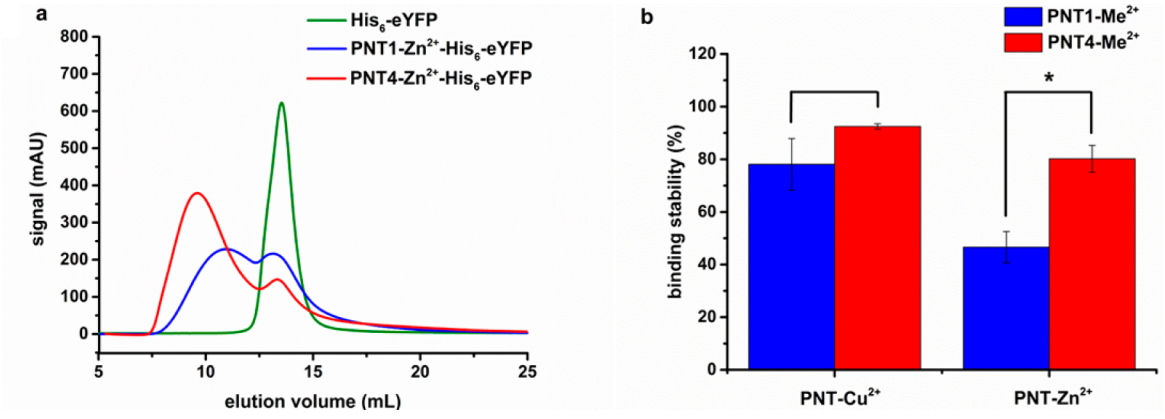

Figure 4. Stability of PNT*n*-Me^{2+}-His_6-eYFP conjugates at pH 7.4. (a) FPLC chromatograms of His_6-eYFP and PNT1/4-Zn^{2+}-His_6-eYFP. (b) Percentage of His_6-eYFP bound with PNT1/4-Me^{2+}. Stars indicate significance in two-tailed Student's *t* test: ∗, $P < 0.05$, $n = 3$.

DOI: 10.1021/acs.jpcb.5b06637
J. Phys. Chem. B 2015, 119, 12066−12073

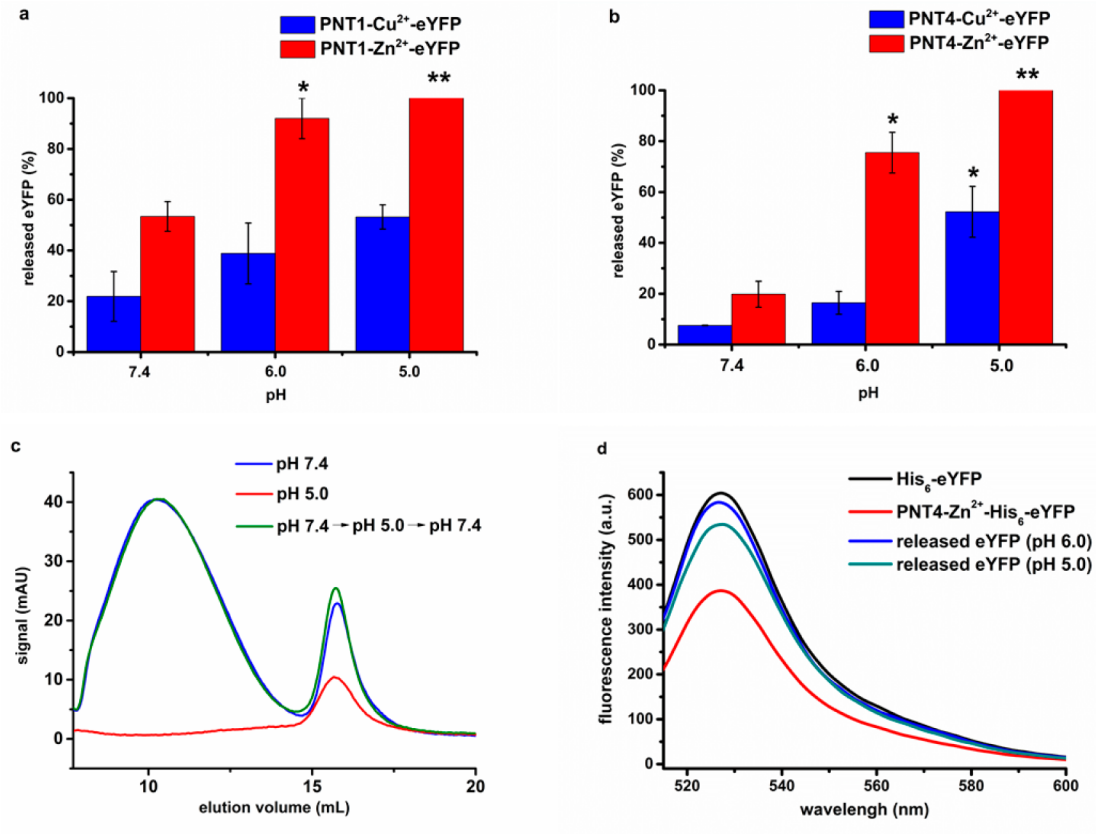

Figure 5. Release of His_6-eYFP from PNT1-Me^{2+} (a) and PNT4-Me^{2+} (b) at different pH values. All statistics were analyzed by comparing samples to their respective protein−polymer conjugate at pH 7.4. Stars indicate significance compared to the equivalent protein polymer conjugate at pH 7.4 in a two-tailed Student's *t* test: ∗, $P < 0.05$; ∗∗, $P < 0.005$. (c) Reversibility of pH dependent binding between PNT4-Zn^{2+} and His_6-eYFP analyzed by FPLC. (d) Fluorescence emission spectra of His_6-eYFP and PNT4-Zn^{2+}-His_6-eYFP before and after release in acidic conditions. Although reactions were run in acidic conditions, all samples were analyzed at pH 7.4 in PBS.

eYFP. Even with a 5-fold increase in potential interaction sites, the % of free protein remained the same, suggesting that the phenomena was caused by interaction with the column (Figure S7). The higher stability of PNT4-Me^{2+}-His_6-eYFP compared to PNT1-Me^{2+}-His_6-eYFP is attributed to interprotein interactions preventing the disassociation of the complex, in agreement with the binding affinity values. Interprotein interactions stabilize the protein−polymer conjugates when the number of trisNTA groups is increased (PNT4 compared with PNT1), strengthening the interaction when the metal is not a strong coordination center (Zn^{2+}).

An attractive property of NTA-Me^{2+}-His_6 molecular recognition is pH sensitive binding.[18] However, this property has previously not been proven with trisNTA-Me^{2+}-His_6. To investigate the pH sensitive binding, a model peptide, hexahistidine labeled with Rhodamine B (RHB-His_6) was used to compare the parameters that effect binding stability across various pHs. RHB-His_6 is strongly quenched when bound to Cu^{2+}, and more stable than eYFP at lower pH.[40] The binding of trisNTA-Cu^{2+} to RHB-His_6 resulted in a significant decrease of fluorescent intensity from 570 to 60. The fluorescent intensity remained unchanged at all pH >3.5 (Figure S8), indicating that the binding between trisNTA-Cu^{2+} and RHB-His_6 is stable at various pHs. PNT4-Cu^{2+}-RHB-His_6 exhibited no dissociation with pH >3.5, suggesting that the presence of polymer does not significantly influence the binding stability. Also, PNT4-Cu^{2+} did not show a significant release of His_6-eYFP when the pH was changed from 7.4 to 6.0, but 52% of the conjugates disassociated at pH 5.0 (Figure 5). As expected, due to the lack of interprotein interactions, the release of His_6-eYFP was more pronounced for PNT1-Cu^{2+} at pH values down to 6, ending at pH 5 to a similar fraction of dissociated conjugates (53%). The higher percent of pH-trigged dissociation can be attributed to the higher K_D at pH 7.4 of PNT4-Cu^{2+}-His_6-eYFP (K_D = 0.36 μM) compared with PNT4-Cu^{2+}-RHB-His_6 (K_D = 0.13 μM).[20] In contrast with PNT*n*-Cu^{2+}, both PNT1-Zn^{2+} and PNT4-Zn^{2+} exhibited a more rapid dissociation. At pH 7.4 PNT1-Zn^{2+} and PNT4-Zn^{2+} dissociated from His_6-eYFP at 53.4% compared to 19.8% determined by FPLC, respectively. Decreasing the pH to 6.0 increased the dissociation of His_6-eYFP from PNT1-Zn^{2+} and PNT4-Zn^{2+} to 92% and 76%, respectively, with both conjugates being completely unbound by pH 5.0 (Figure 5a,b). The higher dissociation of PNT*n*-Zn^{2+}-His_6-eYFP compared with PNT*n*-Cu^{2+}-His_6-eYFP at lower pH was expected, due to the higher K_D values (0.46−1.35 μM, 0.09−0.39 μM, respectively). The trisNTA-Cu^{2+} binding sites on PNT*n* have stronger interactions with His_6-eYFP compared with protons ($K_D \approx 1$ μM);[18,41] therefore, it is difficult to be protonated to induce the dissociation of the proteins. However, the affinity of trisNTA-Zn^{2+} on PNT*n* to His_6-eYFP is comparable to that of protons, resulting in direct competition between protonation and coordination of the His_6-eYFP. This led to PNT*n*-Zn^{2+}-His_6-eYFP having a higher amount of pH-trigged release than PNT-Cu^{2+}-His_6-eYFP. Furthermore, the reversibility of pH dependent binding of PNT4-Zn^{2+}-His_6-eYFP was investigated due to

DOI: 10.1021/acs.jpcb.5b06637
J. Phys. Chem. B 2015, 119, 12066−12073

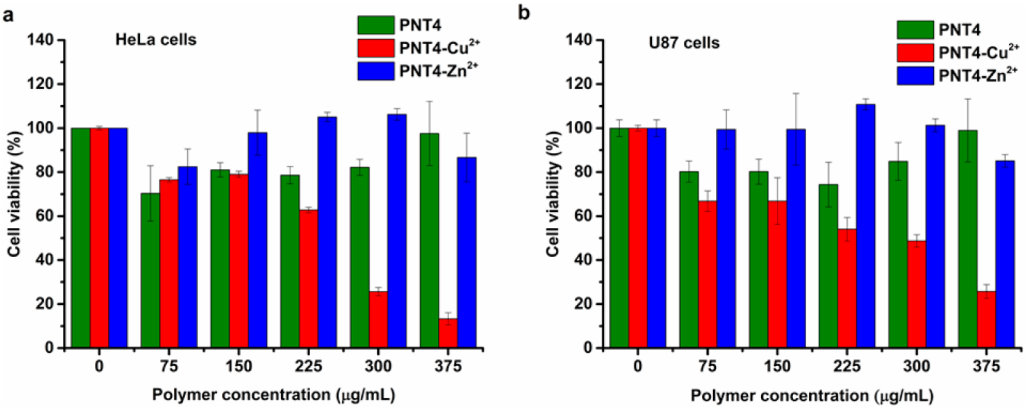

Figure 6. Toxicity evaluation of PNT4-Me^{n+} copolymers on HeLa (a) and U87 (b) cells using MTS assay where zero polymer concentration refers to the addition of PBS to the cells. Errors bars represent the standard deviation (n = 3).

its higher pH binding dependence. A solution of PNT4-Zn^{2+}-His_6-eYFP was formed in pH 7.4 and tested for stability; the pH was then decreased to 5.0 and dissociation was observed. However, when the pH was increased back to pH 7.4 almost complete re-formation of all protein complexes was observed (Figure 5c).

To address the question of whether the reversible binding of PNTn copolymers to His_6-eYFP influences its fluorescent property, His_6-eYFP was characterized by fluorescence spectroscopy before and after polymer conjugation (Figure 5d). When His_6-eYFP was conjugated with PNT4-Zn^{2+}, a decrease in fluorescence intensity was observed due to the chelation with Zn^{2+}. After dissociation from PNT4-Zn^{2+} in acidic conditions (pH 5.0 or 6.0), the released His_6-eYFP was collected and then buffered back to pH 7.4, the fluorescence of His_6-eYFP recovered almost to its original value. The slight decrease of fluorescence intensity was due to short-term exposure to acidic condition which corresponds to literature precedence.[42] In addition, the second structure of dissociated His_6-eYFP after buffering back pH 7.4 was evaluated by CD spectroscopy. No obvious change of the spectrum was observed, suggesting His_6-eYFP was kept intact during the pH-triggered dissociation (Figure S9). Therefore, PNTn copolymers are able to bind His_6-eYFP at physiological pH and release the bound protein in acidic conditions without influencing the structure and properties.

Cytotoxicity Evaluation of PNT4-Me^{n+} Copolymers. The cytotoxicity of PNT4-Me^{n+} copolymers was evaluated on U87 and HeLa cells by using the MTS assay (Figure 6). PNT4 copolymer showed low toxicity in all range of concentrations tested in both cell lines. The coordination of PNT4 with Zn^{2+} did not induce toxicity in contrast to PNT4 coordinated with Cu^{2+} or Ni^{2+} that showed toxicity with increasing concentrations (Figure S10). trisNTA coordinated with Cu^{2+}, Ni^{2+}, Zn^{2+} was tested as a control and showed slightly higher toxicity compared to equivalent copolymer samples (Figure S10). Repeat administrations of Cu^{2+} or Ni^{2+} can accumulate in the liver, kidney, and spleen, leading to organ damage after the complex has dissociated and the metal released.[43−46] Therefore, in terms of its low toxicity, a protein−polymer conjugate composed of PNT4 and Zn^{2+} would be suitable for further in vitro studies.

CONCLUSION

An efficient method to site-specifically and reversibly bind multiple proteins per polymer chain using trisNTA-Me^{2+}-His_6 molecular recognition was designed. His_6-eYFP was used as a model protein for binding PNT-Me^{n+} copolymers. It was demonstrated that the nature of the Me^{n+} and the number of metal binding pockets of trisNTA enable great selectivity for the binding affinity. This led to control of the stability and pH-triggered release of the protein from the polymer by modulating interprotein interactions. After complete release of His_6-eYFP from PNT-Me^{2+} copolymers at selective pH, the return of fluorescence suggested that the protein was intact and maintained its properties. In addition, the toxicity problem of trisNTA-Me^{n+} and its derivatives has been improved by using Zn^{2+}, which still maintained the binding with His_6-eYFP due to controllable interprotein interactions.

The presented system advances the field from covalent single protein−polymer conjugates to noncovalent multiple protein−polymer conjugates that can be readily formed and dissociated dependent on pH and serves as a platform for the combination of various active agents into one nanosystem to potentially fulfill multiple tasks such as therapy and diagnosis in a combined manner.

ASSOCIATED CONTENT

Supporting Information

The Supporting Information is available free of charge on the ACS Publications website at DOI: 10.1021/acs.jpcb.5b06637.

ITC thermograpms and titration curves, size distributions, TEM image, CD spectra of His_6-eYFP, FPLC chromatograms, fluorescent spectra of trisNTA-Cu^{2+}-RHB-His_6 at various pH, additional cell toxicity data, characteristics of protein−polymer conjugates (PDF)

AUTHOR INFORMATION

Corresponding Authors

*C. G. Palivan. Tel: +41 (0)61 267 38 39. Fax: +41 (0)61 267 38 55. E-mail: cornelia.palivan@unibas.ch.

*W. Meier. Tel: +41 (0)61 267 38 02. Fax: +41 (0)61 267 38 55. E-mail: wolfgang.meier@unibas.ch.

Notes

The authors declare no competing financial interest.

DOI: 10.1021/acs.jpcb.5b06637
J. Phys. Chem. B 2015, 119, 12066−12073

■ ACKNOWLEDGMENTS

We thank Swiss National Science Foundation and University of Basel for financial support. J.L. thanks the China Scholarship Council for supporting the fee to study abroad. We thank Biozentrum Biophysics Facility Basel for the use of their ITC instrument. J.L. thanks Mariana Spulber from University of Basel for extensive discussions.

■ REFERENCES

(1) Leader, B.; Baca, Q. J.; Golan, D. E. Protein Therapeutics: a Summary and Pharmacological Classification. *Nat. Rev. Drug Discovery* **2008**, *7*, 21−39.
(2) Frokjaer, S.; Otzen, D. E. Protein Drug Stability: a Formulation Challenge. *Nat. Rev. Drug Discovery* **2005**, *4*, 298−306.
(3) De Groot, A. S.; Scott, D. W. Immunogenicity of Protein Therapeutics. *Trends Immunol.* **2007**, *28*, 482−490.
(4) Duncan, R. Polymer Conjugates as Anticancer Nanomedicines. *Nat. Rev. Cancer* **2006**, *6*, 688−701.
(5) Knop, K.; Hoogenboom, R.; Fischer, D.; Schubert, U. S. Poly(ethylene glycol) in Drug Delivery: Pros and Cons as Well as Potential Alternatives. *Angew. Chem., Int. Ed.* **2010**, *49*, 6288−6308.
(6) Kolate, A.; Baradia, D.; Patil, S.; Vhora, I.; Kore, G.; Misra, A. PEG - aVersatile Conjugating Ligand for Drugs and Drug Delivery Systems. *J. Controlled Release* **2014**, *192*, 67−81.
(7) Pelegri-O'Day, E. M.; Lin, E.-W.; Maynard, H. D. Therapeutic Protein−Polymer Conjugates: Advancing Beyond PEGylation. *J. Am. Chem. Soc.* **2014**, *136*, 14323−14332.
(8) Harris, J. M.; Chess, R. B. Effect of Pegylation on Pharmaceuticals. *Nat. Rev. Drug Discovery* **2003**, *2*, 214−221.
(9) Gauthier, M. A.; Klok, H.-A. Polymer-Protein Conjugates: an Enzymatic Activity Perspective. *Polym. Chem.* **2010**, *1*, 1352−1373.
(10) Secundo, F. Conformational Changes of Enzymes upon Immobilisation. *Chem. Soc. Rev.* **2013**, *42*, 6250−6261.
(11) Filpula, D.; Zhao, H. Releasable PEGylation of Proteins with Customized Linkers. *Adv. Drug Delivery Rev.* **2008**, *60*, 29−49.
(12) Tao, L.; Liu, J.; Xu, J.; Davis, T. P. Bio-Reversible polyPEGylation. *Chem. Commun.* **2009**, 6560−6562.
(13) Gong, Y.; Leroux, J.-C.; Gauthier, M. A. Releasable Conjugation of Polymers to Proteins. *Bioconjugate Chem.* **2015**, *26*, 1172.
(14) Kulkarni, S.; Schilli, C.; Grin, B.; Müller, A. H. E.; Hoffman, A. S.; Stayton, P. S. Controlling the Aggregation of Conjugates of Streptavidin with Smart Block Copolymers Prepared via the RAFT Copolymerization Technique. *Biomacromolecules* **2006**, *7*, 2736−2741.
(15) Chen, J.; Zhao, M.; Feng, F.; Sizovs, A.; Wang, J. Tunable Thioesters as "Reduction" Responsive Functionality for Traceless Reversible Protein PEGylation. *J. Am. Chem. Soc.* **2013**, *135*, 10938−10941.
(16) Kim, T. H.; Swierczewska, M.; Oh, Y.; Kim, A.; Jo, D. G.; Park, J. H.; Byun, Y.; Sadegh-Nasseri, S.; Pomper, M. G.; Lee, K. C.; et al. Mix to Validate: a Facile, Reversible PEGylation for Fast Screening of Potential Therapeutic Proteins In Vivo. *Angew. Chem., Int. Ed.* **2013**, *52*, 6880−6884.
(17) Nguyen, T. H.; Kim, S.-H.; Decker, C. G.; Wong, D. Y.; Loo, J. A.; Maynard, H. D. A Heparin-Mimicking Polymer Conjugate Stabilizes Basic Fibroblast Growth Factor. *Nat. Chem.* **2013**, *5*, 221−227.
(18) June, R. K.; Gogoi, K.; Eguchi, A.; Cui, X.-S.; Dowdy, S. F. Synthesis of a pH-Sensitive Nitrilotriacetic Linker to Peptide Transduction Domains to Enable Intracellular Delivery of Histidine Imidazole Ring-Containing Macromolecules. *J. Am. Chem. Soc.* **2010**, *132*, 10680−10682.
(19) André, T.; Reichel, A.; Wiesmüller, K.-H.; Tampé, R.; Piehler, J.; Brock, R. Selectivity of Competitive Multivalent Interactions at Interfaces. *ChemBioChem* **2009**, *10*, 1878−1887.
(20) Liu, J.; Spulber, M.; Wu, D.; Talom, R. M.; Palivan, C. G.; Meier, W. Poly(N-Isopropylacrylamide-co-Tris-Nitrilotriacetic Acid Acrylamide) for a Combined Study of Molecular Recognition and Spatial Constraints in Protein Binding and Interactions. *J. Am. Chem. Soc.* **2014**, *136*, 12607−12614.
(21) Lata, S.; Reichel, A.; Brock, R.; Tampé, R.; Piehler, J. High-Affinity Adaptors for Switchable Recognition of Histidine-Tagged Proteins. *J. Am. Chem. Soc.* **2005**, *127*, 10205−10215.
(22) Grunwald, C.; Schulze, K.; Reichel, A.; Weiss, V.; Blaas, D.; Piehler, J.; Wiesmüller, K.; Tampé, R. In Situ Assembly of Macromolecular Complexes Triggered by Light. *Proc. Natl. Acad. Sci. U. S. A.* **2010**, *107*, 6146.
(23) Huang, Z.; Hwang, P.; Watson, D. S.; Cao, L.; Szoka, F. C. Tris-Nitrilotriacetic Acids of Subnanomolar Affinity Toward Hexahistidine Tagged Molecules. *Bioconjugate Chem.* **2009**, *20*, 1667−1672.
(24) Nehring, R.; Palivan, C. G.; Casse, O.; Tanner, P.; Tu xen, J.; Meier, W. Amphiphilic Diblock Copolymers for Molecular Recognition: Metal-Nitrilotriacetic Acid Functionalized Vesicles. *Langmuir* **2009**, *25*, 1122−1130.
(25) Broyer, R. M.; Grover, G. N.; Maynard, H. D. Emerging Synthetic Approaches for Protein-Polymer Conjugations. *Chem. Commun.* **2011**, *47*, 2212−2226.
(26) Bolanos-Garcia, V. M.; Wu, Q.; Ochi, T.; Chirgadze, D. Y.; Sibanda, B. L.; Blundell, T. L. Spatial and Temporal Organization of Multi-Protein Assemblies: Achieving Sensitive Control in Information-Rich Cell-Regulatory Systems. *Philos. Trans. R. Soc., A* **2012**, *370*, 3023−3039.
(27) Nussinov, R.; Jang, H. Dynamic Multiprotein Assemblies Shape the Spatial Structure of Cell Signaling. *Prog. Biophys. Mol. Biol.* **2014**, *116*, 158−164.
(28) Saka, S. K.; Honigmann, A.; Eggeling, C.; Hell, S. W.; Lang, T.; Rizzoli, S. O. Multi-Protein Assemblies Underlie the Mesoscale Organization of the Plasma Membrane. *Nat. Commun.* **2014**, *5*, 4059.
(29) Bruns, N.; Pustelny, K.; Bergeron, L.; Whiehead, T.; Ckark, D. Mechanical Nanosensor Based on FRET Within a Thermosome: Damage-Reporting Polymeric Materials. *Angew. Chem., Int. Ed.* **2009**, *48*, 5666−5669.
(30) Griffith, B. R.; Allen, B. L.; Rapraeger, A. C.; Kiessling, L. L. A Polymer Scaffold for Protein Oligomerization. *J. Am. Chem. Soc.* **2004**, *126*, 1608−1609.
(31) Saluja, A.; Kalonia, D. S. Nature and Consequences of Protein−Protein Interactions in High Protein Concentration Solutions. *Int. J. Pharm.* **2008**, *358*, 1−15.
(32) Van Rijn, P. Polymer Directed Protein Assemblies. *Polymers* **2013**, *5*, 576−599.
(33) Cairo, W. C.; Gestwicki, E. J.; Kanai, M.; Kiessling, L. L. Control of Multivalent Interactions by Binding Epitope Density. *J. Am. Chem. Soc.* **2002**, *124*, 1615−1619.
(34) Choe, W.-S.; Clemmitt, R. H.; Chase, H. A.; Middelberg, A. P. J. Comparison of Histidine-Tag Capture Chemistries for Purification Following Chemical Extraction. *J. Chromatogr. A* **2002**, *953*, 111−121.
(35) Stadlbauer, S. Coordination Chemistry in Molecular Recognition. *Ph.D. Dissertation*, University of Regensburg, Regensburg, 2009.
(36) Xia, Y.; Tanga, S.; Olsen, B. D. Site-Specific Conjugation of RAFT Polymers to Proteins via Expressed Protein Ligation. *Chem. Commun.* **2013**, *49*, 2566−2568.
(37) Pujar, N. S.; Zydney, A. L. Electrostatic Effects on Protein Partitioning in Size-Exclusion Chromatography and Membrane Ultrafiltration. *J. Chromatogr. A* **1998**, *796*, 229−238.
(38) Arakawa, T.; Ejima, D.; Li, T. S.; Philo, J. S. The Critical Role of Mobile Phase Composition in Size Exclusion Chromatography of Protein Pharmaceuticlas. *J. Pharm. Sci.* **2009**, *99*, 1674−1692.
(39) Stulik, K.; Pacaova, V.; Ticha, M. Some Potentialities and Drawbacks of Contemporary Size-Exclusion Chromatography. *J. Biochem. Biophys. Methods* **2003**, *56*, 1−13.
(40) Lata, S.; Gavutis, M.; Tampé, R.; Piehler, J. Specific and Stable Fluorescence Labeling of Histidine-Tagged Proteins for Dissecting Multi-Protein Complex Formation. *J. Am. Chem. Soc.* **2006**, *128*, 2365−2372.
(41) Liu, T.; Ryan, M.; Dahlquist, F. W.; Griffith, O. H. Determination of pKa Values of the Histidine Side Chains of Phosphatidylinositol-Specific Phospholipase C from Bacillus Cereus by

DOI: 10.1021/acs.jpcb.5b06637
J. Phys. Chem. B 2015, 119, 12066−12073

NMR Spectroscopy and Site-Directed Mutagenesis. *Protein Sci.* **1997**, *6*, 1937−1944.
(42) Anderson, D. E.; Becktel, W. J.; Dahlquist, F. W. pH-Induced Denaturation of Proteins: a Single Salt Bridge Contributes 3−5 kcal/mol to the Free Energy of Folding of T4 Lysozyme. *Biochemistry* **1990**, *29*, 2403−2408.
(43) Turnlund, J. R. Human Whole-Body Copper Metabolism. *Am. J. Clin. Nutr.* **1998**, *67*, 960S−964S.
(44) Pereira, M. C.; Pereira, M. L.; Sousa, J. P. Evaluation of Nickel Toxicity on Liver, Spleen, and Kidney of Mice after Administration of High-Dose Metal Ion. *J. Biomed. Mater. Res.* **1998**, *40*, 40−47.
(45) Gupta, S. Cell Therapy to Remove Excess Copper in Wilson's Disease. *Ann. N. Y. Acad. Sci.* **2014**, *1315*, 70−80.
(46) Guo, H.; Wu, B.; Cui, H.; Peng, X.; Fang, J.; Zuo, Z.; Deng, J.; Wang, X.; Deng, J.; Yin, S.; et al. $NiCl_2$-Down-Regulated Antioxidant Enzyme mRNA Expression Causes Oxidative Damage in the Broiler's Kidney. *Biol. Trace Elem. Res.* **2014**, *162*, 288−295.

DOI: 10.1021/acs.jpcb.5b06637
J. Phys. Chem. B 2015, 119, 12066−12073